69th International Astronautical Congress, Bremen, Germany 1-5. October 2018 ,

IAC–18–C3.3.5

An Energy Management Approach for Satellites

Tobias Posielek[a]*

[a] *Institute of System Dynamics and Control, DLR German Aerospace Center, Münchener Straße 20, 82234 Weßling, Germany,* tobias.posielek@dlr.de
* Corresponding Author

The energy system is a major factor influencing the design process of a satellite. Improvements of the energy system may reflect in a reduction of mass and costs. DLRbat is a project of the German Aerospace Center investigating energy storages in order to improve the energy system. One main goal of the project is to develop a methodology to design mission specific batteries. As battery durability is one critical factor for space applications, the design of a battery management system is necessary. Furthermore, the usage of additional supercapacitors is incorporated into the design. Within the scope of this project is also the development of an intelligent energy management algorithm. A typical viable satellite configuration for an energy management consists of multiple variable power sources and electric loads. While solar panels act as a viable power source during the time the satellite is not in eclipse, energy storages such as batteries and supercapacitors may act as source as well as loads. Other electric loads such as heaters can be controlled to obtain an optimal power efficiency. In this paper, all of these mentioned components are incorporated into an energy management design, to allow an optimal usage of each individual component. To do so, the Modelica modelling language is used to describe the full satellite dynamics. The energy system is described by various power generators, converters and electric loads. As the power efficiency and durability of a electric component varies with temperature, a thermal system is modelled to monitor the temperatures of each individual component. The energy management optimises the battery durability and reduction of peak loads by exploiting the properties of the different power sources and the thermal inertia. Simulations are carried out to verify the proposed design. The simulation of the complete satellite system incorporating the electrical as well as the thermal system and its dynamics, enables maximal optimisation potential in comparison to conventional methods and speeds up the design process.

1. Introduction

Energy management leads to an optimisation of the amount of energy which will be produced or consumed by components of an electrical system. This concept is exploited in many different applications such as hybrid vehicles [1–6] or electric aircraft [7–11]. Energy management is also favourable in the context of spacecraft in order to optimise the battery lifetime and the usage of battery, supercapacitors and heaters. In [12] the feasibility of supercapacitors for micro-satellites is analysed in order to allow operating high power demanding payloads while enhancing battery life time. Energy management has been investigated in the context of braking energy recovery by [13]. The energy-efficient satellite routing problem is defined in [14] and algorithms are given to prolong the battery lifetime significantly. In [15] a combination of a worst case static solution and a dynamic scheme are proposed to optimise the load task rewards while meeting deadlines and not depleting the energy budget. In [16] the offline design and online management of satellite power systems is discussed. For both of these, a critical state of charge is determined to guarantee that power shortages of the subsystems do not occur. Each load has different versions which need different amounts of power. A dynamic algorithm is proposed which finds the highest possible version while guaranteeing no power shortage.

In this paper, the complete electrical system is modelled including solar panels, batteries, supercapacitors, heaters and various other electrical loads. These use the spacecraft, sun and earth position as well as the temperature evolution in the satellite. Detailed models describing these dynamics are given and an energy management is designed to control these components. The energy management focuses on the distribution of power generated and demanded by the solar array, battery, supercapacitors and electric loads such as heaters or actuators. We assume the existence of sufficient power to fully charge the battery in each orbit after eclipse so that the task can

be formulated as a stationary optimisation problem. We use a market model based algorithm to solve this optimisation problem. The rest of the paper is organised as follows: Section 2 gives an overview about the modelling of the complete system, in Section 3 the market management algorithm is described, in Section 4 a mission example is simulated, and finally, in Section 5, we summarise the presented results and give an outlook on future research.

2. Modelling

Figure 1 depicts the partition of the total system into different subsystems. The energy management uses information of all the other system in order to determine the individual power that shall be produced or consumed by the electrical components. In this paper, the main focus lies on the modelling of the energy system and the energy management. The spacecraft dynamics include mainly the attitude dynamics and the orbit kinematics based on the gravity field. Details of these and its implementation can be found in [17] and [18], respectively.

2.1 The Electric System

Many of the components of the electric system of a spacecraft can also be found in a high-altitude solar-powered aircraft. Thus, some of the models described take a similar form as in previous work described in [19] and [20].

Solar Panels

The solar panels may be modelled as an electrical equivalent circuit as described in [21]. However, we use an ideal diode which is why no leakage losses to the ground and series losses are assumed. The equivalent circuit can be seen in Figure 2, where parameters can be fitted using common solar panel datasheets such as [22]. The diode current I_d is described by

$$I_\mathrm{d} = I_\mathrm{ds}(e^{\frac{V_\mathrm{d}}{V_\mathrm{t}}} - 1)\,, \tag{1}$$

where I_ds is the saturation current of the diode, V_t the thermal voltage and V_d the voltage across the diode. This leads to the load current

$$I = I_\mathrm{L} - I_\mathrm{ds}(e^{\frac{V_\mathrm{d}}{V_\mathrm{t}}} - 1)\,, \tag{2}$$

where I_L is the current produced due to the irradiation. This current is a function of the angle ϕ_ps between the solar panel normal and the sun as well as the distance r_ps from solar panel to sun such that

$$I_\mathrm{L} = \max\left(0, G_{s0}\nu\left(\frac{r_\mathrm{s}}{r_\mathrm{ps}}\right)^2 \cos\phi_\mathrm{ps}\right)\,, \tag{3}$$

where G_{s0} denotes the solar constant, r_s the distance between earth and sun and ν a shadow function modelling the spacecraft eclipse due to earth [23].

Common datasheets such as [22] provide the open circuit voltage V_oc, the short current I_sc and the maximum power point voltage V_mp and current I_mp. All of these are modelled as a linear function of the temperature T which take the form

$$V_\mathrm{oc}(T) = V_\mathrm{oc0} + (T - T_0)dV_\mathrm{oc} \tag{4}$$

where V_oc0 and T_0 describe the reference open circuit voltage and temperature and dV_oc the change of voltage over the temperature. These can be used to determine the diode parameters

$$I_\mathrm{ds} = I_\mathrm{sc}e^{-\frac{V_\mathrm{oc}}{V_\mathrm{t}}}\,, \tag{5a}$$

$$V_t = \frac{V_\mathrm{mp} - V_\mathrm{oc}}{\ln\frac{I_\mathrm{mp}-I_\mathrm{sc}}{I_\mathrm{sc}}}\,. \tag{5b}$$

For N_s solar panels in series and N_p panels in parallel, the resulting array can be modelled as a single panel with the parameters

$$I_\mathrm{ds}^\mathrm{arr} = N_\mathrm{p}I_\mathrm{sc}e^{-\frac{N_\mathrm{s}V_\mathrm{oc}}{V_\mathrm{t}}}\,, \tag{6}$$

$$V_\mathrm{t}^\mathrm{arr} = V_\mathrm{t}N_\mathrm{s}\,, \tag{7}$$

$$I_\mathrm{L}^\mathrm{arr} = N_\mathrm{p}I_\mathrm{L}\,, \tag{8}$$

where $\cdot^\mathrm{arr}$ denotes the array cell solar panel parameter.

In order to obtain the desired power, the solar panel is connected to a DC/DC-converter with the desired voltage. The equivalent circuit can be seen in Figure 3. Usually, this converter is used as a maximum power point tracker in order to obtain the maximal producible power. The produced power P can be determined by

$$P = V_\mathrm{d}\left(I_\mathrm{L} - I_\mathrm{ds}\left(e^{\frac{V_\mathrm{d}}{V_\mathrm{t}}} - 1\right)\right)\eta \tag{9}$$

where η is the total efficiency incorporating losses according to [24] due to cells mismatch $\eta_\mathrm{CM} = 0.99$, parameter calibration $\eta_\mathrm{PC} = 0.97$, UV and micrometeorite effects $\eta_\mathrm{AD} = 0.9975$. Additionally, the efficiency due to diode losses η_DI is modelled such that

$$\eta = \eta_\mathrm{CM}\,\eta_\mathrm{PC}\,\eta_\mathrm{AD}\,\eta_\mathrm{DI}\,. \tag{10}$$

In order to obtain the maximum power, the derivative of P with respect to the terminal voltage $V = V_\mathrm{d}$ is calculated:

$$\frac{dP}{dV} = (I_\mathrm{L} + I_\mathrm{ds} - I_\mathrm{ds}e^{\frac{V}{V_\mathrm{t}}}\left(1 + \frac{V}{V_\mathrm{t}}\right))\eta\,. \tag{11}$$

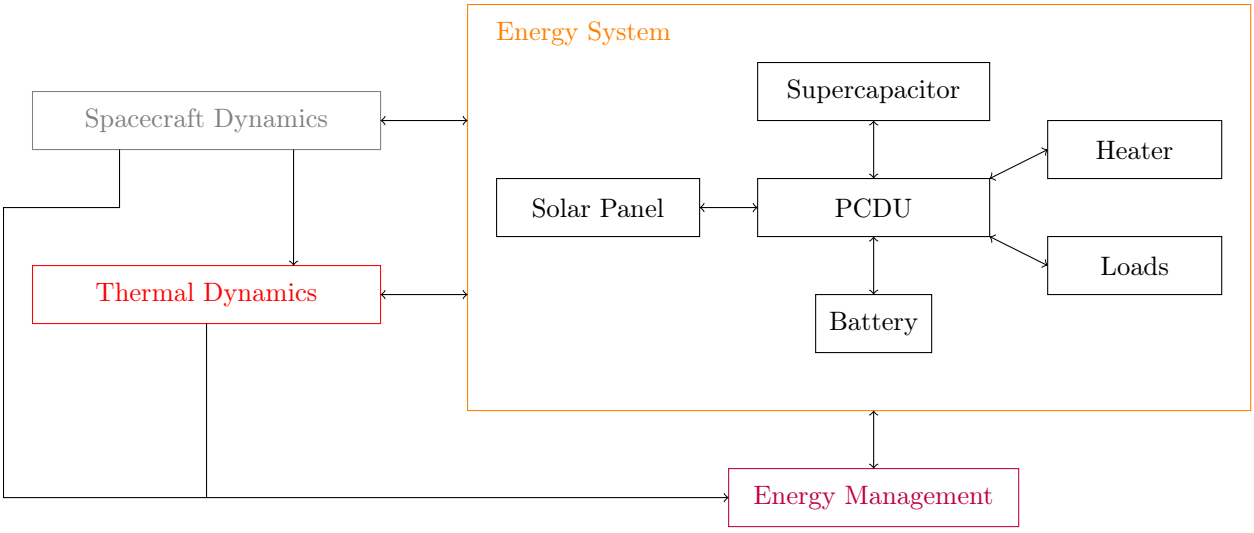

Fig. 1: Total model of the spacecraft system

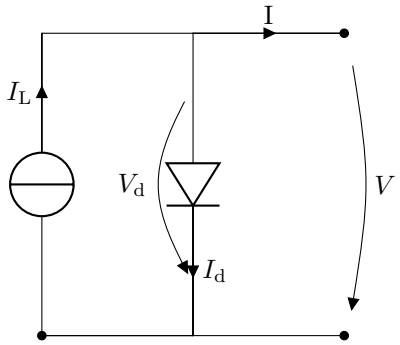

Fig. 2: Electric Circuit representing Solar Panel

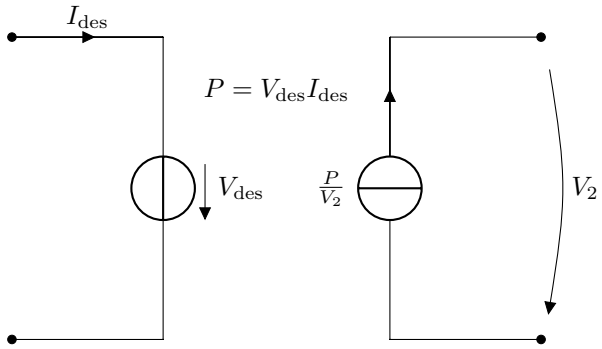

Fig. 3: DC/DC converter connected to Solar Panel

This equation may now be solved numerically with $\frac{dP}{dV} = 0$ for V in order to obtain the maximum power point voltage V_{des}. Note that due to numerical inaccuracies and the neglection of losses, this optimal voltage does not necessarily match the manufacturer's values V_{mp}.

In other scenarios, such as if the battery is fully charged, it is necessary that the solar array produces not maximal but a smaller desired amount of power. This is realised by solving Equation (9) numerically to obtain the desired voltage V_{des} of the DC/DC converter.

Battery

The equivalent circuit for the battery can be seen in Figure 4 similar to [21]. It consists of a voltage source V_{oc} and an inner resistance R_{i}. Additionally, each battery has a capacity C determining the amount of electric charge it can deliver. These parameters can be obtained from a datasheet such as [25]. The voltage V_{oc} is a function of the State of Charge SoC and the Temperature T. Note that the effect of temperature will be disregarded in this paper. The state of charge is determined by the amount of capacity remaining in the battery over the rated capacity [21], i.e.

$$SoC(t) = \frac{\int_0^t I(t)\mathrm{dt}}{C}\,. \tag{12}$$

A typical curve describing the nonlinear dependency of V_{oc} over SoC can be found in Figure 5. Note the cut-off voltage when the battery is almost depleted. For a battery pack with N_{s} cells in series and N_{p} cells in parallel the pack may be modelled as a single

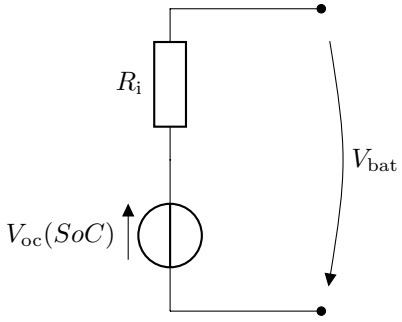

Fig. 4: Electric Circuit representing Battery

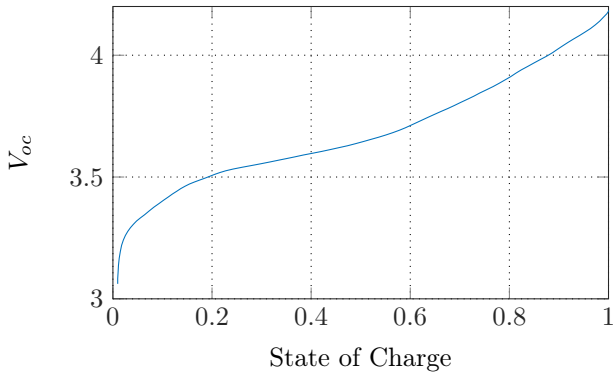

Fig. 5: Open Circuit Voltage over State of Charge of a Battery

battery with

$$R_i^{\mathrm{pack}} = \frac{N_\mathrm{s}}{N_\mathrm{p}} R_\mathrm{i}\,, \tag{13a}$$

$$V_\mathrm{oc}^{\mathrm{pack}} = N_\mathrm{s} V_\mathrm{oc}^{\mathrm{si}}\,, \tag{13b}$$

$$C^{\mathrm{pack}} = N_\mathrm{p} C^{\mathrm{si}}\,, \tag{13c}$$

where $\cdot^{\mathrm{arr}}$ denotes battery pack parameter.

Supercapacitors

A simple model of a supercapacitor can be seen in Figure 6. It consists of a capacitor with a resistor in series. The performance of the capacitor is determined by the resistance R, the capacity of the capacitor C and the rated voltage V_r which can be obtained from datasheets such as [26]. The State of Charge of the supercapacitor can be easily calculated as it is proportional to the capacitor voltage

$$SoC = \frac{V_\mathrm{C}}{V_\mathrm{r}}\,. \tag{14}$$

Again for N_s supercapacitor in series and N_p in parallel Equation (13) is used. Supercapacitors are mainly

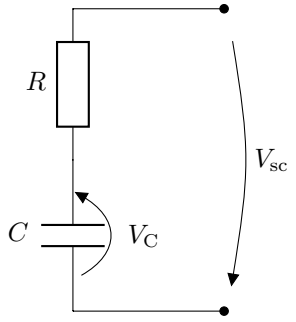

Fig. 6: Supercapacitor equivalent Circuit

used in order to reduce the load peaks which might damage the battery.

Electric Loads

Every component which draws an amount of electric power is modelled as an electric load. This includes heaters, attitude actuators and payloads of the satellite with time dependent schedule. An electric load can simply be modelled as a current source which implements the desired power P_des with $I_\mathrm{des} = \frac{P_\mathrm{des}}{V}$. However, this implementation is not always sufficient, especially when such a load is connected to the battery. Then the desired current is the solution of the quadratic equation

$$P_\mathrm{des} = -I_\mathrm{des}^2 R + V_\mathrm{oc} I_\mathrm{des} \tag{15}$$

obtained by using Kirchhoff's voltage law. The solution takes the form

$$I_\mathrm{des} = \frac{V_\mathrm{oc}}{2R} \pm \sqrt{\frac{V_\mathrm{oc}^2}{4R^2} - \frac{P_\mathrm{des}}{R}} \tag{16}$$

and

$$V = \frac{V_\mathrm{oc}}{2} \pm \sqrt{\frac{V_\mathrm{oc}^2}{2} - 2P_\mathrm{des}R}\,. \tag{17}$$

Thus, the existence and uniqueness of the solution is in general not guaranteed. The maximum power P_max which can be generated is

$$P_\mathrm{max} = \frac{V_\mathrm{oc}^2}{4R}\,. \tag{18}$$

This corresponds to the voltage of the current source

$$V = \frac{V_\mathrm{oc}}{2}\,. \tag{19}$$

In order to ensure the existence of the solution, a minimal voltage V_min has to be specified. If the voltage

of the source is smaller than this threshold the load acts as a resistor, i.e.

$$I = \begin{cases} \frac{P}{V_{\min}{}^2} V & \text{for } V < \mathrm{V}_{\min} \\ \frac{P}{V} & \text{for } V \geq \mathrm{V}_{\min}\,. \end{cases} \tag{20}$$

In the battery case, uniqueness of the solution can only be guaranteed if $V_{\min} = \frac{V_{\mathrm{oc}}}{2}$. However, if the energy management is carefully designed, the load will only demand the amount of power which is available.

Power Conditioning and Distribution Unit

The power conditioning and distribution unit is the connecting element between all the electrical sources, storages and loads. It incorporates the efficiency of the DC/DC converter η_{MPPT}, the power distribution unit η_{PDU} and the battery recharge efficiency η_{Bat}. The power charged or discharged from the battery P_{Bat} is a result of the conservation of power between the solar array power P_{sa}, the total power demanded by the satellite equipment P_{sat} and the supercapacitor charge or discharge power P_{sc}

$$P_{\mathrm{Bat}} = \begin{cases} P_{\mathrm{Diff}} & \text{if } P_{\mathrm{diff}} > 0 \\ P_{\mathrm{Diff}}\eta_{\mathrm{Bat}} & \text{if } P_{\mathrm{diff}} \leq 0 \end{cases}, \tag{21}$$

where

$$P_{\mathrm{Diff}} = P_{\mathrm{sa}} + \frac{P_{\mathrm{sat}}}{\eta_{\mathrm{PDU}}} + P_{\mathrm{sc}}\,. \tag{22}$$

2.2 Thermal System

Knowledge about the temperature evolution of the spacecraft is essential for the satellite design as well as the expected life time and performance of its components. A detailed derivation of the thermal models can be found in [23]. The main heat flows acting on the spacecraft are direct solar radiation Q^{sun}, albedo Q^{alb}, infrared planetary radiation Q^{pl} and radiation to deep space. These heat flows are described as

$$Q^{\mathrm{sun}} = \begin{cases} \alpha G_s \left(\frac{\|s-r\|}{1\,\mu\mathrm{a}}\right) A\cos\left(\phi\right)\nu & 0 < \phi < \frac{\pi}{2} \\ 0 & \frac{\pi}{2} < \phi < \pi \end{cases}, \tag{23}$$

$$Q^{\mathrm{alb}} = \begin{cases} \rho_{\mathrm{alb}}\alpha G_s(d) A F_{\mathrm{form}}\cos\left(\xi\right) & 0 < \xi < \frac{\pi}{2} \\ 0 & \frac{\pi}{2} < \xi < \pi \end{cases}, \tag{24}$$

$$Q^{\mathrm{pl}} = \varepsilon A F_{\mathrm{form}}(r,n)\sigma T_p^4\,, \tag{25}$$

where α denotes the solar absorptance of the surface, s the position of sun, r the spacecraft position, A the area of the surface, $\phi = \phi(n,r,s) \in [0,\pi]$ the angle between the surface normal and the sun, $\nu = \nu(r,s) \in [0,1]$ the shadow coefficient. Note that the intensity of the solar irradiation varies with the distance as $G_s(d) = G_{s0}d^2$, where d is the distance between spacecraft and sun. For the albedo flux, $\rho_{\mathrm{albedo}} \in [0,1]$ is the albedo coefficient, $\xi(s,r) \in [0,\pi]$ the solar zenith angle and a form factor $F_{\mathrm{form}}(r,n)$ describing the part of the radiation that actually strikes the spacecraft surface. T_p denotes the black body temperature of the earth, σ the Stefan-Boltzmann constant and ε the infra-red emissivity of the surface. The dynamics of the temperature T at a specific surface may be described by the differential equation

$$C\dot{T} = Q^{\mathrm{alb}} + Q^{\mathrm{sun}} + Q^{\mathrm{pl}} - \varepsilon A\sigma T^4 + Q^{\mathrm{r}}\,, \tag{26}$$

where Q^{r} describes the dissipative energy produced by the electrical components. All power lost at the power distribution unit or demanded by electrical loads is converted to dissipative heat Q^{r}. Note that some parameters such as the solar absorptance of the surface α may change over the course of a mission [27]. Thus, satellites are designed such that the temperatures at the end of life are still within an acceptable range. This however, may lead to undesirable low temperatures at the beginning of life which is why additional heaters in early stages of the mission are used. The battery is modelled as a thermal capacitance as well. Between the satellite surface and the battery a thermal resistance is assumed. All dissipative heat is acting on the spacecraft surface while the heat of the heater acts directly on the battery component.

3. Market Management

The market management approach solves the problem describing the optimal power distribution between a number of given energy sources, storages and loads. This approach defines a price to power function $h_i : \nu \to h_i(\nu)$ for each electric component $i \in \mathbb{N}$. This function associates every price ν to an amount of power $h_i(\nu)$ raised or demanded by the electrical component. We declare that produced power renders $h_i(\nu)$ positive while demanded power yields a negative $h_i(\nu)$. This price to power function is the main design parameter of the optimisation problem and reflects whether the component is an electrical source, load or energy storage. Further, the price to power function describes the priority and the efficiency of the electric component. In order to find the optimal energy distribution, an equilibrium between the produced and consumed power has to be

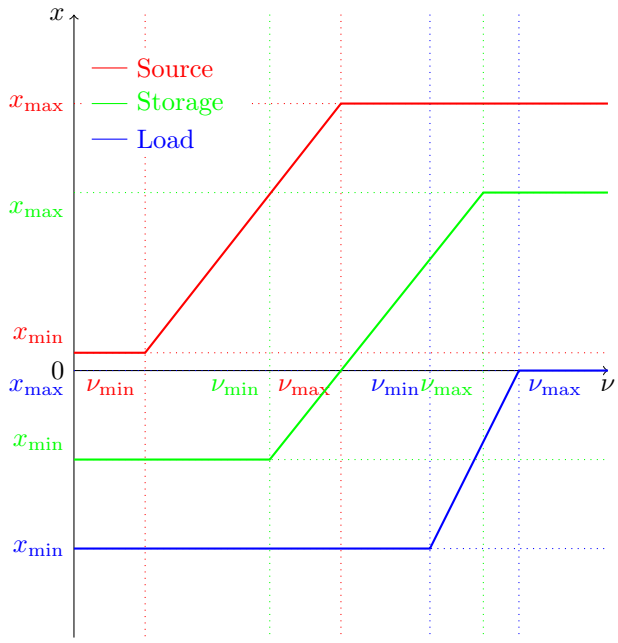

Fig. 7: Graph of a typical Eletric Source, Load and Storage

calculated by

$$\sum_{i=0}^{n} h_i(\nu_i) = 0 \ , \tag{27a}$$

$$\nu_1 = \nu_2 = \ldots = \nu_n = \nu \ . \tag{27b}$$

Of course, the choice of h has to guarantee the existence and ideally the uniqueness of such an equilibrium. This can be ensured by the intermediate value theorem if h_i are chosen as continuous, monotonous functions such that

$$\sum_{i=0}^{n} h_i(0) < 0 < \lim_{\nu \to \infty} \sum_{i=0}^{n} h_i(\nu) \, . \tag{28}$$

This condition implies the intuitive assumption that at a price of zero, all loads obtain maximal power while all sources produce minimal power. In this case, more power can be produced than it is demanded resulting in a negative power balance. On the other side, for an infinitely high price all loads consume only minimal power while all sources produce maximal power. In this case, more power is demanded than it can be produced resulting in a positive power balance. In most scenarios, it is sufficient to define each price to power function as a piecewise affine linear function which we will use for electric sources, loads and energy storages. A typical graph of these functions can be seen in Figure 7.

One advantage of this method is the combination of source and load management. The course of the price can be used with the price to power functions as an indicator to evaluate at each point of time how much each individual source, storage or load produces or demands. Additionally, this method allows the implementation of a modular system as each component is described by an individual price to power function and the solution is described by the Equations 27. This makes this method ideal for an object-oriented, equation based modelling language such as Modelica. The implementation is described in [7] and is successfully used in [8] for aircraft electrical systems. In the following, the affine linear cost functions for sources, storages and loads are introduced that will be used for the proposed energy management.

3.1 Sources

A typical electric source may be described by a price to power function $h : \mathbb{R}^{\geq 0} \to \mathbb{R}$ with

$$h(\nu) = \begin{cases} x_{\min}, & \text{for } \nu < \nu_{\min} \\ m(\nu - \nu_{min}) + x_{\min} & \nu_{\min} \leq \nu \leq \nu_{\max} \\ x_{\max}, & \text{for } \nu > \nu_{\max} \end{cases} \tag{29}$$

where $m = \frac{x_{\max} - x_{\min}}{\nu_{\max} - \nu_{\min}}$ with $\nu_{\min} < \nu_{\max}$, $0 \leq x_{\min} \leq x_{\max}$. The choice of such a price to power function is intuitive, as it assumes a minimal and maximal producible power $x_{\min}$ and $x_{\max}$, respectively and a linear dependence of the price and the produced power. The efficiency of the source is associated with the parameter $\nu_{\min}$ where $\nu_{\max}$ describes the linear correlation between price and produced power.

An example price to power function can be found in [8] as

$$h(\nu) = \begin{cases} 0, & \text{for } \nu < \frac{2k}{\eta} \\ \frac{1}{2k}\nu - \frac{1}{\eta} & \frac{2k}{\eta} \leq \nu \leq 2000k + \frac{2k}{\eta} \\ 1000, & \text{for } \nu > 2000k + \frac{2k}{\eta} \end{cases} , \tag{30}$$

where η denotes efficiency and k quadratic losses of the source.

3.2 Loads

A typical electric source may be described by a price to power function $h : \mathbb{R}^{\geq 0} \to \mathbb{R}$ in the same form as in Equation (29) but with $x_{\min} \leq x_{\max} \leq 0$. The main difference is that both maximal and minimal power must be negative, i.e. power must always be consumed and not produced.

3.3 Energy Storages

A typical electric source may be described by a price to power function $h : \mathbb{R}^{\geq 0} \to \mathbb{R}$ in the same form as in Equation (29) but with $x_{\min} \leq 0 \leq x_{\max}$. Again, the main difference to a source and a load is that the minimal power is smaller than zero while the maximal power is bigger than zero, i.e. an energy storage must be able to consume and to produce power dependent on the price equilibrium. The maximal and minimal power to be generated is limited by the State of Charge of the battery. If a critical limit $SoC_{\min}$ or $SoC_{\max}$ is reached, the corresponding minimal or maximal power $x_{\min}$ or $x_{\max}$ is set to zero. Otherwise these powers are determined by the physical limits of the battery or by specifications of the battery management for example to maximise life duration. The current State of Charge is provided by an external model described in Section 12 simulating the dynamic behaviour of the battery.

4. Simulation of an Example Mission

In this section, an example mission is simulated. In the following, the market management implementations of battery and supercapacitor are stated and details about the electrical loads are described. Finally, the simulation results are presented.

4.1 Battery and Supercapacitor

Ideally, battery and supercapacitor complement each other such that the supercapacitor produces high frequency power demands in order to reduce the peak loads acting on the battery while the battery itself provides all the low frequency power demands because it has the higher capacity. Thus, battery and supercapacitors are modelled in the market model sense as a single component. The maximum discharging power $x_{\max}$ of this component is determined by a maximal current of 1C in order to obtain a longer battery cycle lifetime

$$x_{\max} = V_{\text{bat}} \frac{C}{3600} \,. \tag{31}$$

The resulting power x is then filtered in order to obtain a signal x_{LP} without high power peaks

$$X_{\text{LP}}(s) = \frac{1}{sT+1} X \tag{32}$$

where X_{LP} and X denotes the Laplace transformed of signal x_{LP} and x, respectively. This provides the battery power P_{bat} and supercapacitor power P_{sc} with

$$P_{\text{bat}} = x_{\text{LP}} \,, \tag{33}$$

$$P_{\text{sc}} = x - x_{\text{LP}} \,. \tag{34}$$

Critical State of Charges $SoC_{\min}$ and $SoC_{\max}$ of supercapacitor and battery are defined to limit the maximum amount of energy demanded by the energy management to be drained or fed to the energy storages. In case one of the limits is reached, all the energy is fed to the other storage.

4.2 Electric Loads

In Table 1 an overview about the eletrical loads of a Cubesat is given. Each of these loads is provided with its desired power as well as a minimal and maximal price. The prices are designed by the author based on the load priority and the cost an outage would cause. The table describes all necessary loads of the electrical power system, the on-board-computer, the communication system, the attitude orbit and control system, the scalable power system and the payloads. The evolution of the power depends on the individual payload. For most payloads the power demand is assumed to be constant over the course of the mission. This is described by the function $f_{i,\text{const}}$ with $f_{i,\text{const}}(t) = P_i$ for $i \in \mathbb{N}$.

Time Varying Power Payloads

For some payloads the power demand is modelled as a function of time. The payload is switched on after a start time t_1 for a on duration of t_2 seconds. This process is repeated every t_3 seconds. This is described by the function

$$f_{\text{t},i}(t) = \begin{cases} P_i & \text{if } t \in t_1 + kt_3 + [kt_2, (k+1)t_2) \\ & \text{for } k \in \mathbb{N} \\ 0 & \text{otherwise} \end{cases} . \tag{35}$$

We use the notation $t_1 + [t_2, t_3]$ in order to express the interval $[t_1 + t_2, t_1 + t_3]$.

Receiver and Transmitter

The receivers are toggled at a certain latitude. The transmitters are toggled every time the spacecraft passes the latitude ϕ_{gs} of the ground station when latitude ϕ is rising. The state of the receiver can be described by a variable $a \in \{0, 1\}$ which corresponds to a boolean variable which describes whether the receiver is on or off. This state changes every time a rising edge is detected in $\phi > \phi_{\text{gs}}$, i.e. define the discontinuous function b as

$$b(t) = \text{sgn}(\phi(t + \varepsilon) - \phi_{\text{gs}}) \,. \tag{36}$$

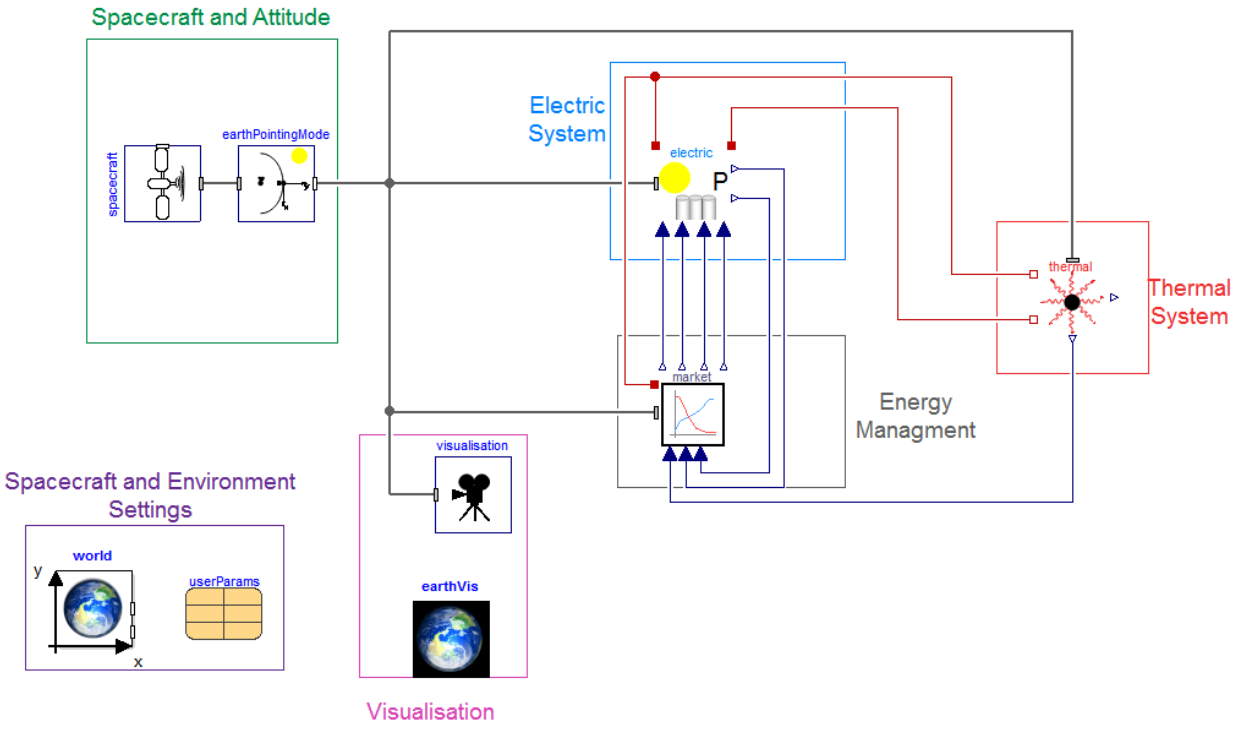

Fig. 8: Modelica Diagram of the Electrical System with Energy Management

Consider a as a boolean variable of time such that

$$a(t) = \begin{cases} a^-(t) & \text{otherwise} \\ \neg a^-(t) & \text{if } b^-(t) < 0 \wedge b(t) \geq 0 \end{cases}, \quad (37)$$

where $a^-(t) := \lim_{\varepsilon \to 0^-} a(t+\varepsilon)$ denotes the left-handed limit of a and

$$\neg a := \begin{cases} 0 & \text{if } a = 1 \\ 1 & \text{if } a = 0 \end{cases}. \quad (38)$$

Additionally, the receivers are operated hot redundant if the satellite passes the ground station which is described by boolean c which is a function of time, i.e. for only small numbers of orbits

$$c(t) = \begin{cases} 1 & \text{if } t \in (t_1, t_2) \\ 0 & \text{otherwise} \end{cases}. \quad (39)$$

Then the requested power is described by

$$f_{\text{rec},i}(t, \phi) = \begin{cases} aP_i & \text{if } c = 0 \\ P_i & \text{if } c = 1 \end{cases}. \quad (40)$$

Heater

A heater for the battery is part of the equipment in order to retain the temperature in a healthy regime for the battery in the early spacecraft orbits. Its power demand is determined based on the current temperature and fed to the energy management. The temperature regime to be maintained is over -2 degree. Thus, a bang bang control law would switches the heater on when the temperature is smaller than -2 degree. In order to avoid chattering during the eclipse, we additionally implement a hysteresis such that the controller switches to the opposite signal only when the deadzone is left. This control law f for the requested power is displayed in Figure 9.

4.3 Simulation

The spacecraft is in a sun synchronous orbit with an altitude of 600km and 06:00h longitude of the ascending node simulated on 2020-06-17 at 09:45h. We have used the proposed models as well as the DLR Environment library [18], the Space Systems library [28] and the Visualization library [29] to implement the example mission. In Figure 8 the high level representation of the Modelica model can be seen, including the different subsystems and the signal flow between them. For example, the energy management uses the State of Charge of the battery and supercapacitor provided by the electric system and delivers reference power signals for solar panels, battery, su-

Electrical Load	Power P_i	Function	Parameter	Minimal Price	Maximal Price
PCDU	1.26	$x = f_{\text{const},1}(t)$		340	350
Battery module 1	0.16	$x = f_{\text{const},2}(t)$		340	350
Battery module 2	0.16	$x = f_{\text{const},3}(t)$		340	350
CMM	2.2	$x = f_{\text{const},4}(t)$		310	320
IFM	1.2	$x = f_{\text{const},5}(t)$		310	320
RXNOM	4.2	$x = f_{\text{rec},6}(t, \phi)$	$\phi_{\text{gs}} = 48$, $t_1 = 22980$, $t_2 = 24000$	300	310
TXNOM	8.4	$x = f_{\text{rec},7}(t, \phi)$	$a = 0$, $t_1 = 22980$, $t_2 = 24000$	300	310
RXRED	4.2	$x = f_{\text{rec},8}(t, \phi)$	$\phi_{\text{gs}} = 48$, $t_1 = 22980$, $t_2 = 24000$	300	310
Sunsensors	0.54	$x = f_{\text{const},9}(t)$		330	340
Magnetometer	0.63	$x = f_{\text{const},10}(t)$		330	340
IMU	2.1	$x = f_{\text{const},11}(t)$		330	340
GPS	1.06	$x = f_{\text{const},12}(t)$		320	330
Torquer Control Unit	2.5	$x = f_{\text{const},13}(t)$		330	340
Reaction Wheels	3.96	$x = f_{\text{cons},14\text{t}}(t)$		200	210
PCDU SPS	1.2	$x = f_{\text{const},15}(t)$		140	150
APR SPS	1.2	$x = f_{\text{const},16}(t)$		140	150
Payload 1 Part 1	0.288	$x = f_{\text{t},17}(t)$	$t_1 = 5460$, $t_2 = 2700$, $t_3 = 23232$	110	120
Payload 1 Part 2	0.504	$x = f_{\text{t},18}(t)$	$t_1 = 5460$, $t_2 = 2700$, $t_3 = 23232$	110	120
Payload 1 Part 3	0.5	$x = f_{\text{t},19}(t)$	$t_1 = 11220$, $t_2 = 2040$, $t_3 = 46464$	110	120
Payload 1 Part 4	1.05	$x = f_{\text{t},20}(t)$	$t_1 = 11220$, $t_2 = 2040$, $t_3 = 46464$	110	120
Payload 1 Part 5	0.084	$x = f_{\text{t},21}(t)$	$t_1 = 17100$, $t_2 = 1980$, $t_3 = 23232$	110	120
Payload 1 Part 6	0.252	$x = f_{\text{t},22}(t)$		110	120
Payload 2 Part 1	0.12	$x = f_{\text{const},23}(t)$		120	130
Payload 2 Part 2	0.24	$x = f_{\text{const},24}(t)$		120	130
Payload 2 Part 3	0.44	$x = f_{\text{const},25}(t)$		120	130
Payload 3	2.3625	$x = f_{\text{t},26}(t)$	$t_1 = 19500$, $t_2 = 600$, $t_3 = 92928$	130	140
Heater	4	$x = f_{\text{const},27}(t)$		340	350

Table 1: Overview of Electrical Loads

percapacitor and loads. The spacecraft is simulated with five solar panels at different sides with each having four cells in series and twelve in parallel. The parameters are based on [22]. A battery with four cells in parallel and four in series is assumed. Its parameters are given by [25]. A pack of three supercapacitors in parallel and nine in series with parameters provided by [26] is chosen.

Nominal Scenario

In the nominal scenario, the energy management is evaluated in view of the overall system dynamics, the power distribution between battery and supercapacitor and the heater activity. Figure 10 shows the total power produced by the solar array, the State of Charge of the battery and the power demanded by the satellite. In the beginning, the solar array produces the maximal possible power to fully charge the battery. After the battery is fully charged, the DC/DC converter controls the solar array to produce only the power necessary for the electrical loads.

Figure 11 shows the price evolution in this scenario. It can be seen that only source management is necessary since enough power can be produced by battery or solar array. There are three different price regimes in this scenario. A low price regime when the satellite is sunlit and the battery is fully charged. A medium price regime when the satellite is sunlit and the battery is charged and a high price regime when the spacecraft is in eclipse and all power has to be raised by the battery. Figure 12 shows the power raised by the battery during eclipse with and with-

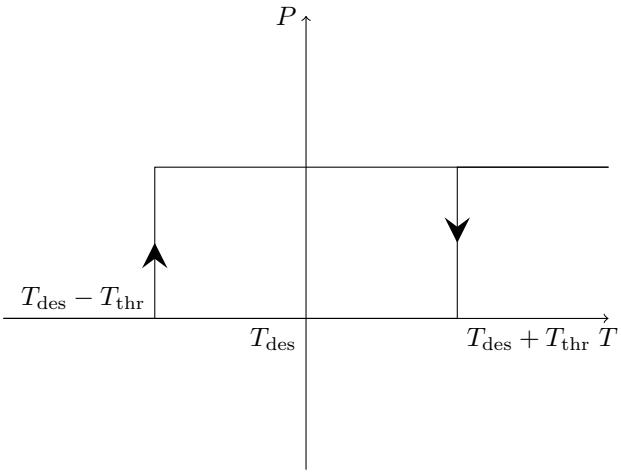

Fig. 9: Heater Control Law

out supercapacitor. The existence of a supercapacitor smoothes the power demand and thus the current signal. A reduction of these current signal peaks may lead to a longer battery life time. Figure 13 shows the temperature evolution in the satellite. It can be observed that the temperature leaves the desired temperature regime if no heater is present. The heater is switched on at the critical temperature to retain the temperature in the desired regime. The heater is switched off if the temperature leaves the deadband again. This leads to a temperature evolution within the deadzone.

Battery Failure Scenario

In this scenario, a battery failure is simulated where only two batteries in parallel and in series are working. This influences the maximal discharge power of the energy storage component. Figure 14 shows the price evolution. While the price looks the same during the phase the satellite is sunlit. The price during eclipse is drastically higher than in the nominal scenario. This is due to the fact that the maximum power which can be produced by the battery without significantly diminishing its lifetime is not sufficient to sustain all loads. Thus, this high price means that all loads with lower maximal price are turned off which is considered as the optimal solution to maximise battery lifetime while also powering high priority loads.

5. Conclusions

In this paper the electrical system of a satellite is modelled and an energy system using a market model approach is designed to allow an optimal power distribution between the electrical components. Special focus is put on the temperature evolution of critical components. The suggested market model method has proven to be efficient as it combines source and load management. It fulfils the task of power distribution without using predictive information. In future work, methods using predictive algorithms will be introduced and different algorithms to distribute the power between battery and supercapacitor will be analysed.

References

[1] R. E. Araujo et al. “Combined Sizing and Energy Management in EVs with Batteries and Supercapacitors”. In: *Transactions on Vehicular Technology* 63.7 (2014), pp. 3062–3076.

[2] L. Serrao et al. “Optimal energy management of hybrid electric vehicles including battery aging”. In: *American Control Conference*. IEEE, 2011.

[3] L. Tang, G. Rizzoni, and S. Onori. “Energy Management Strategy for HEVs Including Battery Life Optimization”. In: *Transactions on Transportation Electrification* 1.3 (2015), pp. 211–222.

[4] Z. Chen et al. “Optimal Energy Management Strategy of a plug-in Hybrid Electric Vehicle based on a Particle Swarm Optimization Algorithm”. In: *Energies* 8.5 (2015), pp. 3661–3678.

[5] C. Musardo et al. “A-ECMS: An Adaptive Algorithm for Hybrid Electric Vehicle Energy Management”. In: *European Journal of Control* 11.4-5 (2005), pp. 509–524.

[6] T. van Keulen et al. “Energy Management in Hybrid Electric Vehicles: Benefit of Prediction”. In: *IFAC Symposium on Advances in Automotive Control*. Vol. 6. 2010.

[7] D. Zimmer and D. Schlabe. “Implementation of a Modelica Library for Energy Management based on Economic Models”. In: *Proceedings of the 9th International Modelica Conference*. 2012, pp. 133–142.

[8] D. Schlabe. “Modellbasierte Entwicklung von Energiemanagement-Methoden für Flugzeug-Energiesysteme”. PhD thesis. Dresden University of Technology, 2015.

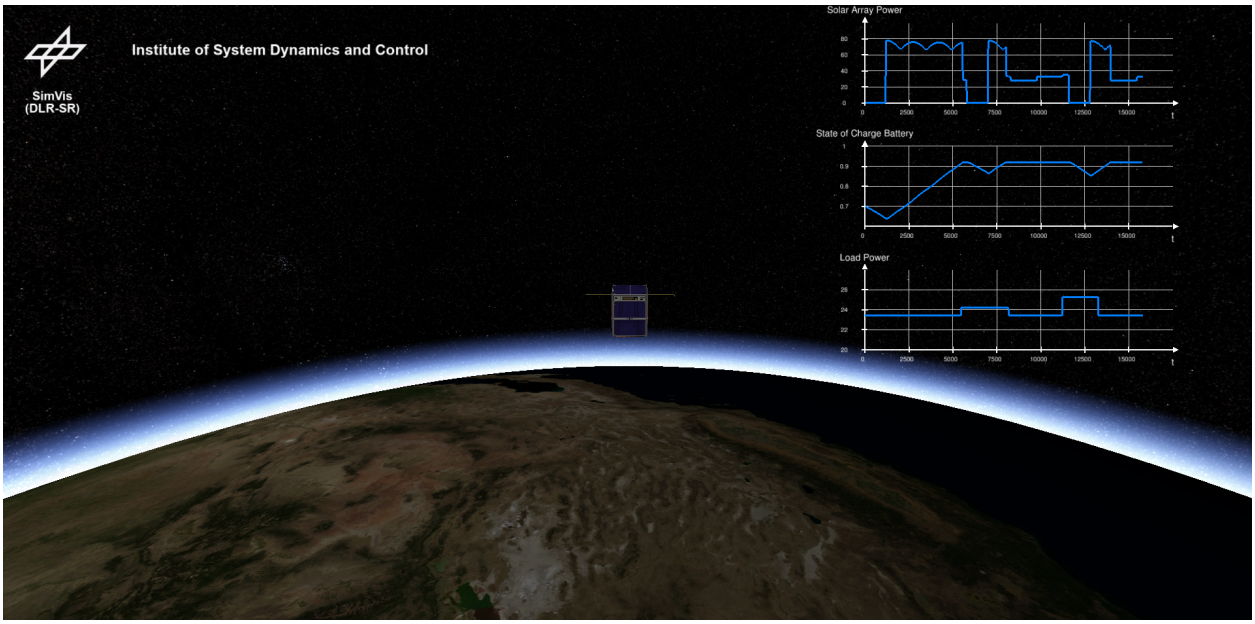

Fig. 10: SimVis visualisation of the Satellite with Electrical System and Energy Management.

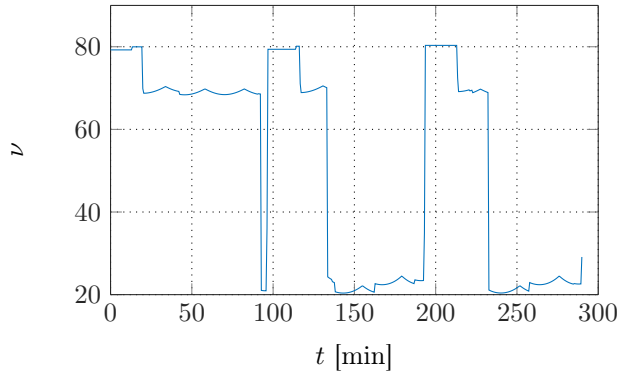

Fig. 11: Price Evolution in the Nominal Scenario.

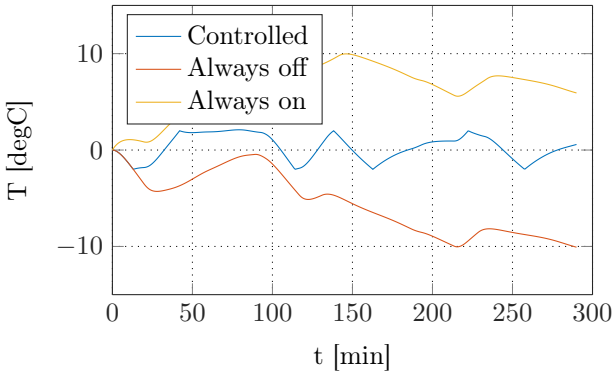

Fig. 13: Temperature Evolution under different Heater Usage

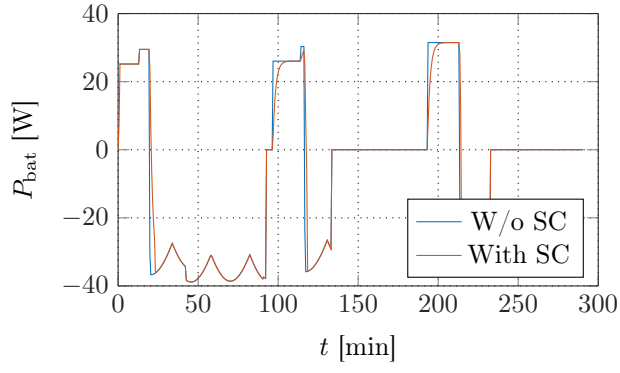

Fig. 12: Power commanded or produced with and without Supercapacitor (SC)

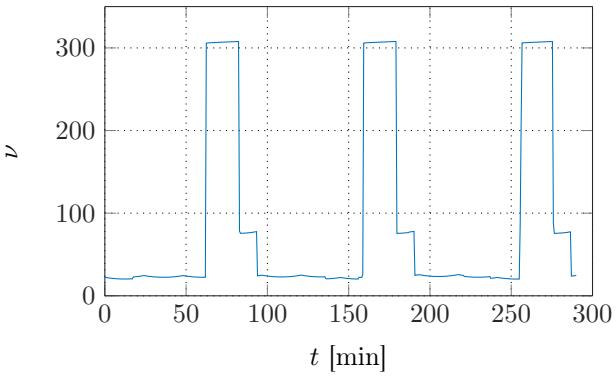

Fig. 14: Price Evolution with Battery Damage

[9] S. N. Motapon, L.-A. Dessaint, and K. Al-Haddad. "A Comparative Study of Energy Management Schemes for a Fuel-Cell Hybrid Emergency Power System of More-Electric Aircraft". In: *Transactions on Industrial Electronics* 61.3 (2014), pp. 1320–1334.

[10] R. Todd et al. "Supercapacitor-Based Energy Management for Future Aircraft Systems". In: *Applied Power Electronics Conference and Exposition*. IEEE. 2010, pp. 1306–1312.

[11] X.-Z. Gao et al. "Energy Management Strategy for Solar-Powered High-Altitude Long-Endurance Aircraft". In: *Energy Conversion and Management* 70 (2013), pp. 20–30.

[12] T. Shimizu and C. Underwood. "Super-Capacitor Energy Storage for Micro-Satellites: Feasibility and Potential Mission Applications". In: *Acta Astronautica* 85 (2013), pp. 138–154.

[13] J. Han et al. "Research on Braking Energy Recovery and Energy Management System for Spacecraft". In: *Transportation Electrification Conference and Expo*. IEEE, 2014.

[14] Y. Yang et al. "Towards Energy-Efficient Routing in Satellite Networks". In: *Journal on Selected Areas in Communications* 34.12 (2016), pp. 3869–3886.

[15] C. Rusu, R. Melhem, and D. Mossé. "Multi-Version Scheduling in Rechargeable Energy-Aware Real-Time Systems". In: *Journal of Embedded Computing* 1.2 (2005), pp. 271–283.

[16] J. Lee, E. Kim, and K. G. Shin. "Design and Management of Satellite Power Systems". In: *Real-Time Systems Symposium*. IEEE. 2013, pp. 97–106.

[17] F. L. Markley and J. L. Crassidis. *Fundamentals of spacecraft attitude determination and control*. Vol. 33. Springer, 2014.

[18] L. E. Briese, A. Klöckner, and M. Reiner. "The DLR Environment Library for Multi-Disciplinary Aerospace Applications". In: *Proceedings of the 12th International Modelica Conference*. 132. 2017, pp. 929–938.

[19] A. Klöckner, D. Schlabe, and G. Looye. "Integrated Simulation Models for High-Altitude Solar-Powered Aircraft". In: *AIAA Modeling and Simulation Technologies Conference*. 2012, p. 4717.

[20] A. Klöckner et al. "Integrated Modelling of an Unmanned High-Altitude Solar-Powered Aircraft for Control Law Design Analysis". In: *Advances in Aerospace Guidance, Navigation and Control*. Springer, 2013, pp. 535–548.

[21] M. Patel. *Wind and Solar Power Systems*. CRC Press, 1999.

[22] *Triple Junction Solar Cell Assembly 3G30C*. AZUR Space. Aug. 2016.

[23] T. Posielek. "A Modelica Library for Spacecraft Thermal Analysis". In: *Proceedings of the 14th International Modelica Conference* (2018). (in press).

[24] W. Ley, K. Wittmann, and W. Hallmann. *Handbook of Space Technology*. Vol. 22. John Wiley & Sons, 2009.

[25] *Nanopower BPX Battery*. GOMSPACE. Aug. 2016.

[26] *Supercapacitor Datasheet*. Nesscap Ultracpacitors. 2014.

[27] W. J. Larson and J. R. Wertz. *Space Mission Analysis and Design*. Springer, 1991.

[28] M. J. Reiner and J. Bals. "Nonlinear Inverse Models for the Control of Satellites with Flexible Structures". In: *Proceedings of the 10th International Modelica Conference*. 096. 2014, pp. 577–587.

[29] T. Bellmann. "Interactive Simulations and Advanced Visualization with Modelica". In: *Proceedings of the 7th International Modelica Conference*. 043. 2009, pp. 541–550.